UPPSALA UNIVERSITET

Elektro-E 24007

Bachelor Thesis 15 hp

June 2024

Non-contact PCB fault detection using magnetic and infrared methods

---

Albin Ekroth, Albin Glanborg, Texas Gullström, Elias Thornemo Chrokate

Faculty of Science and Technology

Uppsala University, Place of publication: Uppsala

Supervisor: Rasmus Hamrén,

Examiner: Mikael Bergkvist

Master's Programme in Electrical Engineering

Non-contact PCB fault detection using magnetic and infrared methods

Albin Ekroth, Albin Glanborg, Texas Gullström, Elias Thornemo Chrokate

Abstract

This thesis aims to further improve non-contact Printed Circuit Board (PCB) fault detection by measuring its heat- and magnetic emissions. Magnetic emissions are measured using Giant magnetoresistance (GMR) sensors and infrared with Infrared-cameras (IR), data is then used to train Artificial Intelligence (AI) models that will determine the functionality of a device under test. Functional devices should emit unique infrared and magnetic waves meaning that if a sensor is sensitive enough, a signature can be obtained. The magnetic signature in this thesis was not obtained due to time restrictions and unforeseen issues that arose at the final build, but the infrared signature was successful and its AI model gave a clear distinction between faulty and functional devices. The method of infrared testing was a cheap and easy method at gaining a PCBs signature but commercialising the method requires a much larger database than that of this thesis. As for the magnetic method, potential is evident and further research is recommended.

Nomenclature and abbreviations

ADC - Analog to Digital Converter

AI - Artificial Intelligence

DNN - Deep Neural Network

DUT - Device under test

GMR - Giant magnetoresistance

GUI - Graphical User Interface

ICT - In circuit testing

IR - Infrared

PCB - Printed circuit board

Table of contents

1. Introduction

As the world evolves and digitalises it becomes more reliant on electrical devices. Almost all devices are built up by Printed Circuit Boards (PCBs). Due to the heavy reliance on these devices it is critical to find new, efficient and cheap ways to both develop the boards as well as verifying their functionality.

Faulty PCBs can be detected in several different ways depending on the structure of the PCB and the resources available to the tester. A frequently used method is called In Circuit Testing (ICT) which is generally quoted to be able to detect nearly 98% of all faults [1]. This method verifies the board by detecting the electrical signals in all nodes and compares it to the ideal values. However, it does require physical access to not only the board, but also every node, which is an increasing issue as PCBs become denser. It typically also requires either an advanced mechanical machine or a human supervisor, both being an expensive factor. It can even damage some components such as sensitive analog circuits and high-speed digital designs[2]. As ICT's reach their limits, advancements in non-contact methods have become more prevalent [3,4,5].

This thesis was made in collaboration with Nordic Electronics Partner (NEP) who provided the equipment and financing as well as valuable feedback to make this thesis possible. A previous master thesis was done on a similar topic [3] with NEP. This thesis is an attempt at improving previous work in non-contact PCB fault detection from magnetic and infrared signatures of a PCB.

2. Background

2.1 Magnetic fields

There are three different sources to a magnetic field; permanent magnets, a changing electric field, or of most significance to this report, an electrical current. Ampere's law shows the relationship between electrical current and a magnetic field.

$$\nabla \times \vec{B} = \mu_0 \vec{J} \qquad (1)$$

It relates an electrical current $\vec{J}$ to a magnetic field $\vec{B}$ that circulates around a closed loop of current. Magnetic fields can also be viewed in different perspectives, the magnetic field strength, known as the H-field, and the magnetic flux density, known as the B-field. The H-field can be interpreted as the magnetic field produced by the current flowing through a wire, while the B-field is the total magnetic field with the addition of the magnetic properties of the materials in the field [6].

2.2 Giant magnetoresistive sensors

Giant magnetoresistive sensors are a common tool for measuring magnetic fields. The sensor's operation is based on the principle of giant magnetoresistance, an effect observed in multiple layers of alternating ferromagnetic and non-magnetic conductive layers. The giant magnetoresistance sensors experience a significant change in electrical resistance as the alignment of the ferromagnetic layers changes. Without an external magnetic field, the magnetic moment of the ferromagnetic layers aligns in an antiparallel configuration, this results in the layers experiencing a high electrical resistance. Applying an external magnetic field aligns the ferromagnetic layers in parallel to each other, decreasing the electrical resistance [7]. The GMR is built up in a wheatstone bridge configuration with two giant magnetoresistors and two shielded resistors that do not get affected by magnetic fields (*figure 1)*.

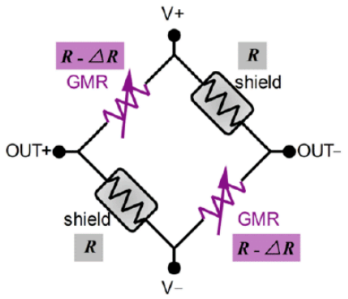

Figure 1: The build up of a GMR, a wheatstone bridge configuration [8]

The output comes in the form of a differential voltage that follows the equations below.

$$V_{out+} = \frac{R}{2R-\Delta R}(V_+ - V_-) + V_- \quad (2)$$

$$V_{out-} = \frac{R-\Delta R}{2R-\Delta R}(V_+ - V_-) + V_- \quad (3)$$

$$V_{out+} - V_{out-} = \frac{\Delta R}{2R-\Delta R}(V_+ - V_-) \quad (4)$$

2.3 IR waves

Infrared waves are a part of the electromagnetic spectrum. Due to its longer wavelength between 780 nm and 1000 μm they are invisible to the human eye, but it is detectable to the skin as heat. The experiment done by William Herschel in 1800 concluded the difference in temperature between the colours in the visible spectrum with temperature increasing from blue to red. This laid the foundation of the technology that has become thermal imaging. Devices such as night vision goggles and thermal cameras allow people to see the IR emissions from objects. [9]

2.4 IR-Sensors

There are two types of IR-sensors, passive IR-sensors (PIR-sensors) and Active IR-sensors, which are both used in different ways.

The active IR-sensors are sending out IR-waves through, most often, an LED and measuring the time for the signal to return. Depending on the strength of the returning wave, it is possible to measure the distance from the object. It is most often used in robotics when measuring distances between objects.

The PIR-sensors change their properties depending on the temperature that it is exposed to. A change in the resistance leads to a change in voltage or current which can be used as a measurable signal to display the temperature in which the IR-sensor detects. Unlike the active IR-sensors, the PIR-sensors do not emit their own IR-waves. [10].

2.5 IR-Cameras

There are two different types of IR cameras, night vision and thermal cameras. The night vision cameras use active IR-sensors which need an external light source that sends out IR-light which in turn will reflect on surfaces. The thermal camera uses the PIR-sensors, therefore it does not need an external light source [11]. In this case, thermal cameras are used for monitoring the temperature of a surface or area without touching it. By creating a matrix of IR-sensitive components inside the lens of the camera, it can create a digital image of the area that is being

measured. The resolution of the camera depends on the size of the IR-component matrix. By using the output voltage of each pixel that corresponds to the pixels measured temperature, a colour map is created which can either be grayscale, which means there are 255 different values for the camera to display, or RGB with 255 different values for the three colors [12]. This means that the Grayscale has a lower range than the RGB-camera.

2.6 Neural networks

Neural networks are machine learning models that mimic the way biological neurons in the brain work together to draw conclusions [13]. In this thesis, a neural network will be the method for pattern recognition in both the IR, and magnetic sensing divisions. A network consists of three types of layers; an input layer, hidden layers, and an output layer. A layer consists of neurons with each playing a role in determining the system's output. In contrast to a digital computer which sends zeros and ones to communicate, neurons send signals that can have any value ranging between 0 and 1, giving it the ability, not only to convey information, but also give an intensity to it. In the case of the input layer, the value of a neuron can be directly linked to a specific variable in the system such as the output voltage of a GMR. The hidden layers then transform data using a series of carefully balanced neurons to create an output that represents the input dataset. The network is tuned by training it with what is referred to as target data, this is input data that has been given a predetermined output, giving the network an understanding of what to look for. The more target data given, the better the system. By introducing a multitude of faulty and functional DUTs to the target data, a neural network can be an efficient tool in detecting faults in a DUT.

3. Problem statement

Since ICT for PCBs is done by measuring electrical signals at different nodes, a lot of information about the DUT is needed. If different devices are used, some form of advanced machine or human supervisor is needed to move the test needles. This process becomes very time inefficient and costly, and since PCBs are becoming denser and components smaller these systems need to be updated frequently. This thesis asks, can non-contact fault detection of PCBs in the form of magnetic and thermal imaging be made to counteract this issue?

3.1 Research questions

The main goal of the thesis is deconstructed into research questions that can be looked into separately in order to make the final goal easier to reach.

1. Can a magnetic signature of a PCB be determined?
2. Can a thermal signature of a PCB be determined?
3. Is it possible to classify the status of a DUT using machine learning with the data from magnetic and thermal signatures?

4. Method

4.1 Methodology

There are two common ways of detecting IR-waves; temperature sensors and thermal cameras. Thermal cameras is the simpler choice when it comes to creating a signature and can be bought at a reasonable price, this is therefore the chosen method. The magnetic signature will be obtained by GMR sensors, laying out multiple in a matrix configuration, similar to the way that was done in [3]; this design showed promise and was also fairly easy to replicate. This leaves room to further improve the preceding designs.

4.2 Design

Once the components are chosen, designs are to be made. The electrical schematic and PCB layout for the magnetic sensor-PCB are constructed using the software KiCad. Test rigs are created for both divisions, which are used to make tests repeatable and reliable, the software used is Blender and the models are 3D printed. As for the neural network, different softwares is used for the different methods, Matlab's Deep learning Toolbox is used for the magnetic data and the library TensorFlow in python is used for the thermal data. The data from each source is different so it must therefore be treated differently.

4.3 Creating and analyzing a database

For a neural network to recognize the status of a DUT, a substantial database of both faulty and functional PCBs is required. The larger the database, the more reliable the system. This thesis uses only one DUT, so to create a large database a make-shift method has to be used. For the IR-method, the DUT is to be photographed multiple times as it is powered up and gets warmer, this creates a broader spectrum of slightly different heat signatures for the functional database. As for faulty devices, pictures of powered off devices will take its place simulating a device drawing no current, a common result of faulty devices. The main focus of the thesis for its magnetic method will be to create a signature unique to a functioning device and a varying database will only make this more difficult. Only the one device will be used in the functioning database and faulty devices are to be simulated by turning it off.

5. Implementation

5.1 Magnetic field sensor

A 4-layer PCB is created to serve as a magnetic field sensing card. The extra layers of copper insulate the GMR sensors from the rest of the circuitry in order to reduce magnetic noise. The magnetic field sensor card can be split into 4 divisions: the power supply, the GMR sensor circuit, the amplifier circuit and the converter, (*figure 2)*.

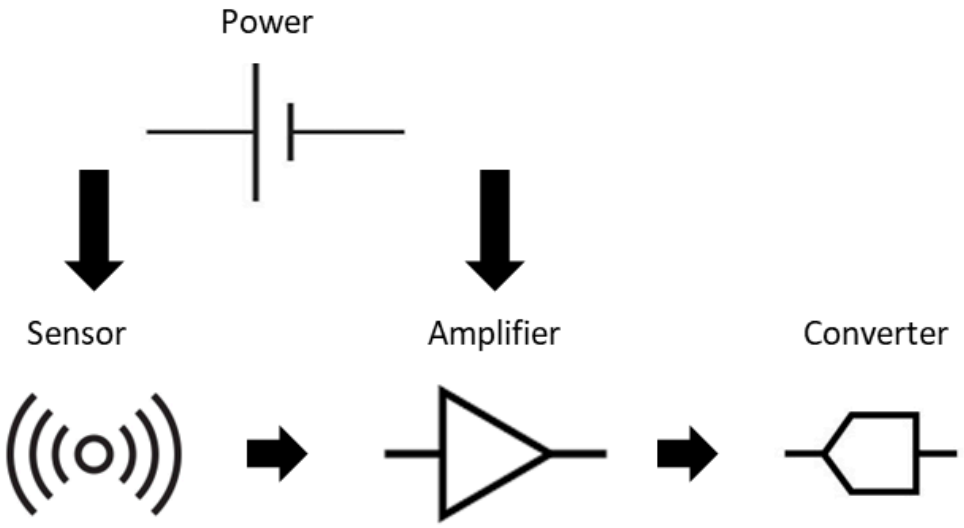

Figure 2: Diagram of the sensor card

5.1.1 GMR sensor circuit

The actual magnetic sensing of the PCB is constructed as a 2x5 matrix of GMR sensors (*figure 3)* and is designed in order to match the size and shape of the DUT, this is to ensure that the magnetic emissions are fully captured. The GMR used is AAH-002E because of its high sensitivity to magnetic fields; a key factor in sensing magnetic fields at a distance, which will be the case when measuring the DUT. A more detailed study went into the best GMR candidate in [3]. A negative trait of the component is the high hysteresis that it comes with, which affects the GMR's output characteristic by creating nonlinearity in the results. To counteract this, a magnetic biassing field is implemented into every GMR by integrating coils at each end of the GMR on its sensitive axis, like the setup used in [14].

According to the datasheet [15], the output of the GMR becomes linear between 0.6Oe to 3Oe, by creating a biassing field that reaches the middle of this range a linear output can be made.

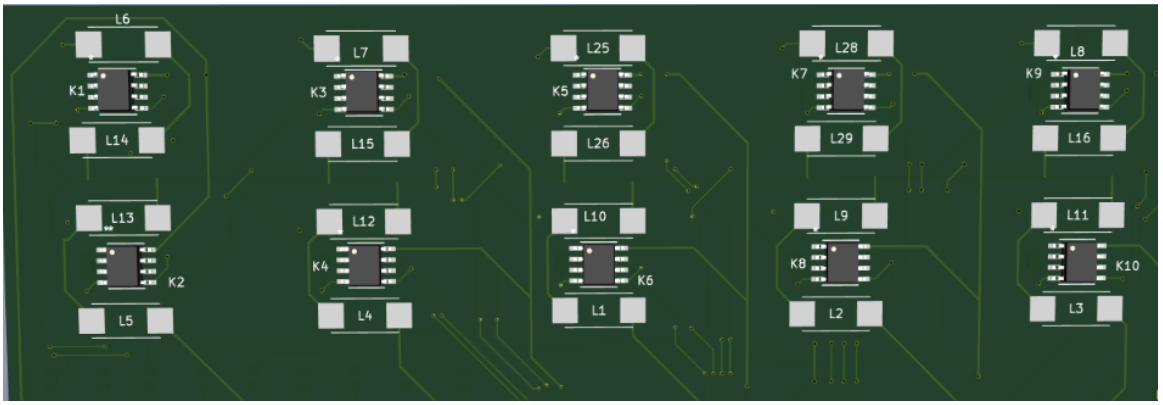

Figure 3: Magnetic sensor circuit with coils integrated at each end of a GMR.

5.1.2 Amplifier circuit

On the other side of the PCB, a 2x5 matrix of instrumental amplifiers is constructed, matching the position of the GMR to shorten the pathway between GMR and the amplifiers since this path is highly susceptible to noise. For this thesis, the INA826 was a recommended choice to the GMR as stated in the GMR's datasheet with the reason of the low component count and excellent common mode rejection ratio [15]. Since the magnetic field strength is thought to vary significantly throughout the DUT, potentiometers are used, allowing for varying amplification for each sensor and maximising the full capabilities of each amplifier. Since the DUT chosen for this thesis functions purely on DC signals, a low pass filter that cuts off most AC signals is implemented. The only signals that should be amplified are the DC signals, however, due to a multitude of possible factors it would be too risky to implement a low pass filter that only lets through pure DC signals.

5.1.3 Converter

In the original work [3] of this thesis, a Teensy 3.6 was used to convert analog to digital signals. The microprocessors sampling rate was too slow for simultaneously collecting data from 16 GMRs, causing signals to become undersampled. The newer model, the Teensy 4.1, has triple the sampling rate at 1MS/s. Also, in this version only 10 GMRs are used, making the Teensy 4.1 satisfactory for the project. Teensy 4.1 is programmed in Arduino IDE. The number of samples taken per test will be determined by making sure the output signals are relatively continuous. To save the data, a program called Coolterm is used, this saves everything that gets printed on the serial monitor on Arduino IDE as a txt file in order to be further processed in Matlab.

5.1.4 Power supply

The GMR sensors and amplifiers require different supply voltages to operate correctly. The GMR is supplied with its maximal supply voltage of 12V [18] which according to *equation 4* will increase the sensitivity. The amplifier is supplied with 3.3V in order to match the teensy's maximum input voltage of 3.3V. To remove unwanted noise from the power supplies, each one is followed by a capacitor multiplier, which acts as a low pass filter, research in [3, p.26] was made to prove the effectiveness of these. The inductors are supplied with enough current to send the GMRs into its linear state, the amount of current required to achieve this is to be examined prior to testing. The AAH002's sensitivity lies between 11 to 18mV per Oersted[18] and since the linear range is in between [0.6, 3]Oe, the GMR's output should lie in between [6.6,54]mV. The coils need to supply a current resulting in a 30.3mV output signal as this puts the GMR in the centre of its linear output range.

5.1.5 Test rig for magnetic sensors

The layout of the test rig for measuring the magnetic signature is a crucial part for the performance of the GMR sensors. To maximise the magnetic sensing capabilities of the GMR, the DUT would have to be as close to the sensors as possible. The smallest distance between the magnetic sensor-PCB and the DUT was 5mm, taking account for the GMR and inductor sizes.

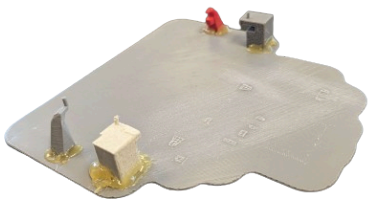

Figure 4: The test rig for sensing the magnetic field.

The two corners were printed for the magnetic sensor card to rest on while the power terminal is meant to stabilise the other side. To keep the DUT in place, pegs were designed on the test rig that go through the device's premade holes.

5.1.6 Neural Network for magnetic testing

The neural networks used in magnetic testing are constructed using the neural network fitting app, found in Matlab's Deep learning toolbox. All of the networks are constructed with 10 input neurons, one neuron for each GMR. To classify the data as faulty or functional, 2 output neurons

are given, [1,0] for functional and [0,1] for a faulty. The network uses Bayesian regularisation and 25 hidden layers for every neural network in order to standardise results.

5.2 IR-camera MLX90640

There are several different cameras that have thermal imaging and that would perform well in this project. One of the major differences when scaling up the price tag of different cameras is the resolution the device can provide. Important to remember is that the objective of this project is not to detect faulty components, but faulty PCBs. Therefore, it is, to some extent, not essential to use the more advanced cameras. MLX90641 has a resolution of 24x32 pixels and is a cheaper option that couples well with a raspberry pi as its controlling unit.

5.2.1 Test rig for IR-camera

In order to use machine learning for image recognition it is crucial that the picture of each DUT is taken under the same circumstances. One solution is to make a specific test rig for the particular DUT which will ensure results, however it would not be possible to test PCBs with different layouts. A variable test rig could be used for several different PCBs, although it risks the board's placement ending up in slightly different places which will, as mentioned, taint the results. With this in mind a semi-variable test rig is used. The camera's height is adjustable depending on the size of the DUT, whereas the platform that holds the DUT in place is specifically designed for each different PCB. The result can be seen in *figure 5*.

Figure 5: The test rig for the IR method.

5.2.2 Raspberry pi

The IR-camera is controlled by a Raspberry Pi 3B. This is a programmable single-board computer and needs an external keyboard, screen, mouse etc. to function as a regular computer. In this case however, a pre-programmed library for a GUI is used which allows the user to access the raspberry pi operating system on an ordinary computer via a screen sharing program.

5.2.2.1 MLX90641 combined with raspberry pi

The raspberry pi unit is only used for taking pictures with the IR-camera. The code written simply takes a picture and saves it to the raspberry pi which is later transferred to the computer where the machine learning is used.

Due to the DUT's components gradually increasing temperature as it is turned on, each picture is ideally taken at the same time after the DUT is powered up. However, since there is limited access to different DUTs, pictures are taken at different times to increase the variety of the database.

5.2.3 Image processing and machine learning

A library called OpenCV is used to process the images. It is one of the largest open-source libraries that is used for processing images to create suitable files that can later be used in machine learning. By using the processed images through OpenCV, the Tensorflow library is used to save the data and create a Deep Neural Network (DNN). When a DUT is photographed, the DNN uses two different databases to compare the image to. One database contains images of faulty PCBs, and the other of functional ones, with both being assigned a number, 0 and 1, respectively. As the image is processed in the algorithm it will print out a decimal number between 0 and 1, depending on how closely it resembles to either database. A rough outline to follow is that any value above 0.5 can be considered a functional PCB and anything below is a faulty PCB. However, since faulty PCBs have different errors, this database is more varying and cannot be relied on the same way. Therefore, a different threshold that is closer to 1 must be set to compensate for this. This limit may vary depending on the design of the PCB. By testing previously known working PCBs a new limit can be set depending on the results. In this case it is set to 0.9.

6. Results

6.1 GMR sensor data

A series of graphs are displayed below that show the output of each GMR from each test. Each GMR in *Figure 6* has a unique colour assigned to it, this will make it easier to recognize patterns that a DUT might have with one another as well as determining the change in activity between faulty and functional devices. Due to lack of time, every faulty DUT was simply turned off, this should at least give the largest distinction between faulty and functional devices. Each result shows 100 samples taken and converted, from bits to millivolts, at 9600 baud. Standardising the conditions for each test was definitely a goal for this thesis but proved to be more difficult than expected. For reasons that are further explained in the discussion section of this report, tests were taken in pairs with the test number indicated in the title of each graph; these pairs are sought to be more standardised than others.

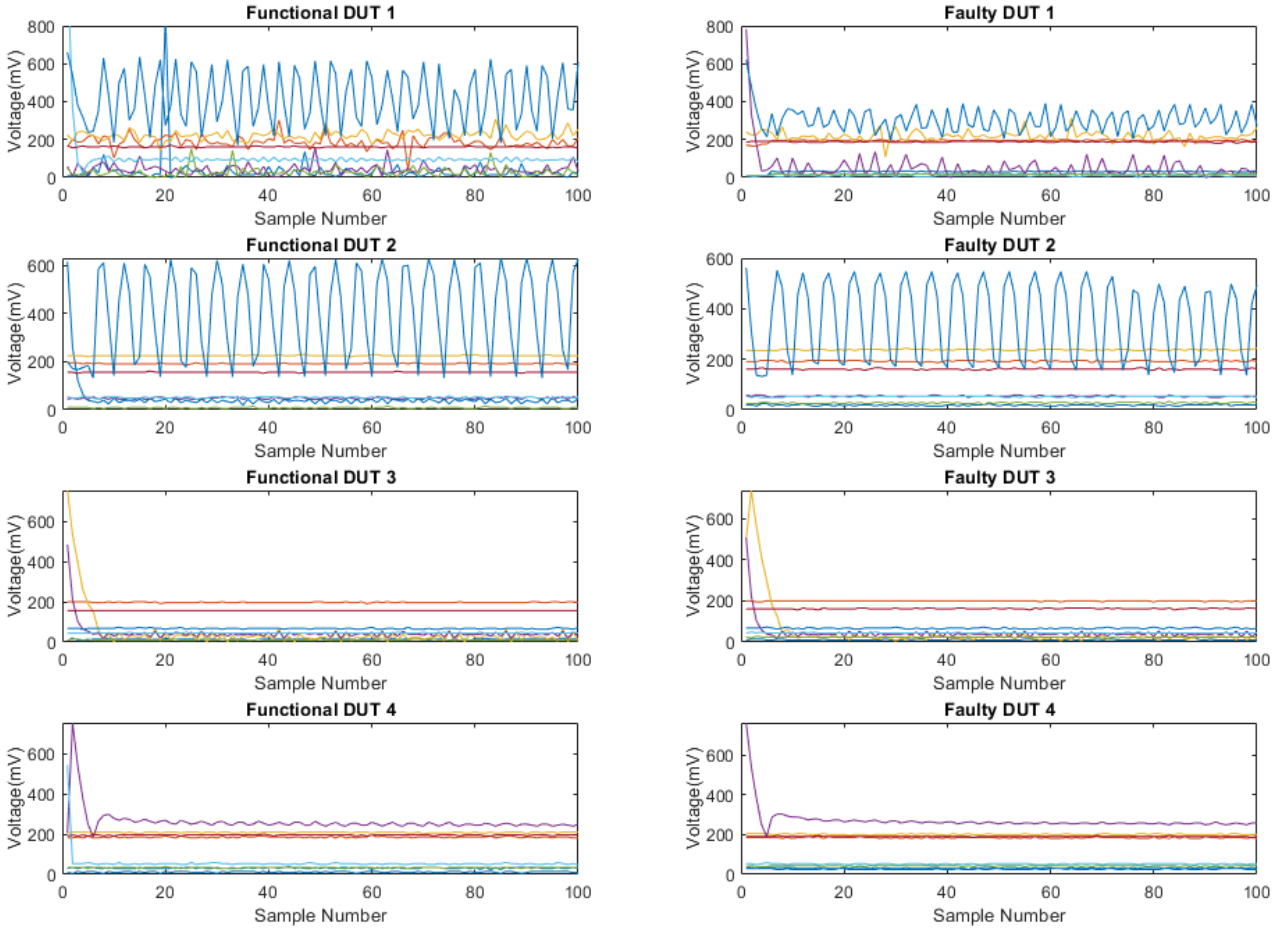

Figure 6:Graphs of the GMR's output signals in each test.

Due to the lack of external noise, Test #3 was chosen for further detailed investigation, as shown in *figure 7* and *figure 8.*

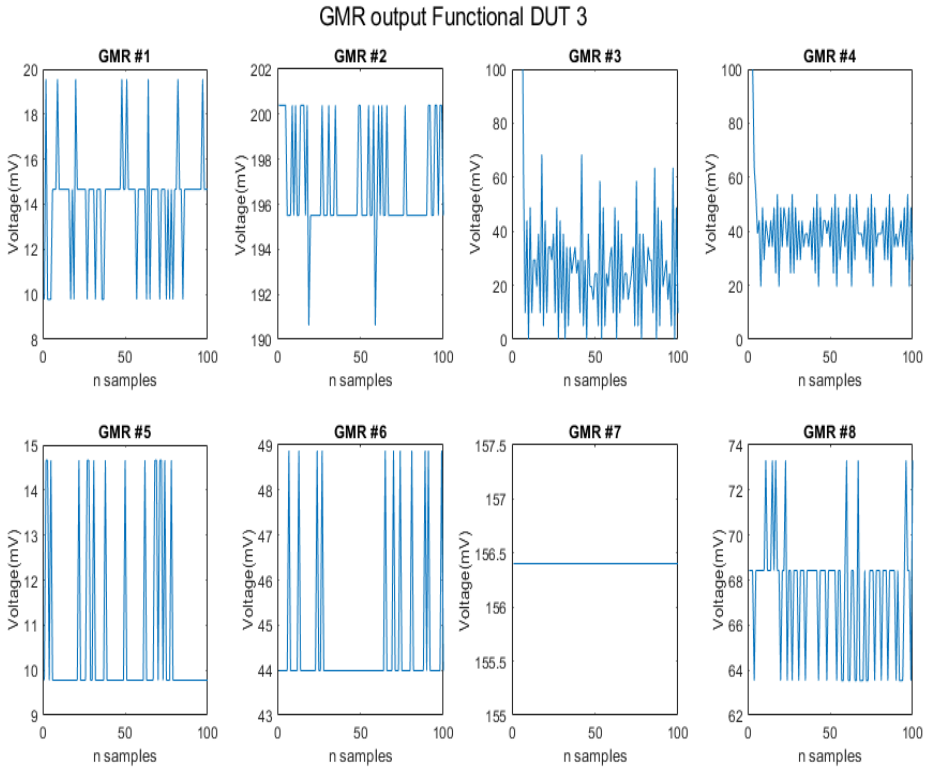

Figure 7: graphs of each sensor output from the third test when measuring a functional DUT.

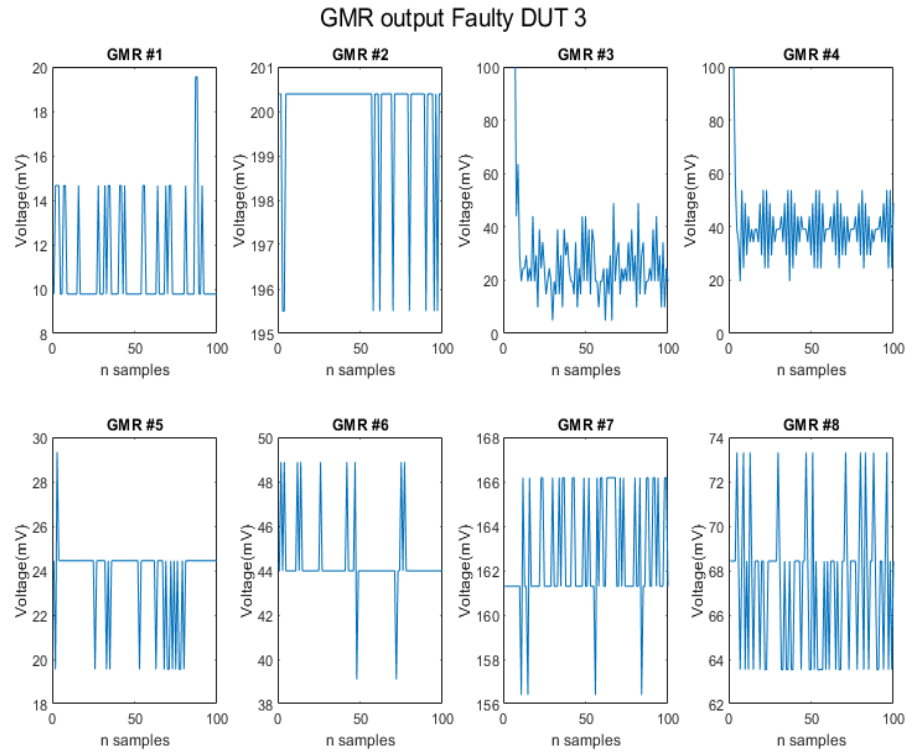

Figure 8: graphs of each sensor output from the third test when measuring a faulty DUT.

Due to the inability to create standardised testing, deducing if a magnetic signature is possible becomes difficult by only looking at the graphs above. To analyse whether a magnetic signature was possible, a differential voltage for each GMR between testing-pairs was looked at.

Table 1: Differential voltage in millivolts for each GMR at each test.

Differential voltage between Faulty and Functional tests [mv]								
Test \ GMR	1	2	3	4	5	6	7	8
1	3.6	8.2	3.8	8	10	83	27	110
2	20	0.88	12	6.3	18	1.3	4.7	47
3	3.2	3.2	1.1	29	13	0.2	6.2	34
4	0.53	0.3	6.7	10.8	10	0.15	4.1	14

Table 2: Neural networks using different variants of training data and tests.

Neural network classification system			
Neural network #	Trainingdata	Results	
1	Faulty 1,2,3 Functional 1,2,3	Faulty 4	[1.2,0.2]
		Functional 4	[1.2,0.2]
2	Faulty 2,3,4 Functional 2,3,4	Faulty 1	[0.9,0.1]
		Functional 1	[0.3,0.7]
3	Faulty 1,3,4 Functional 2,3,4	Faulty 2	[0.1,1.1]
		Functional 1	[0.3,1.3]

6.2 IR-images

Figure 9 is an example photograph of a faulty DUT, which is the DUT turned off. The heat signature is mostly monotone with smaller shifts due to noise.

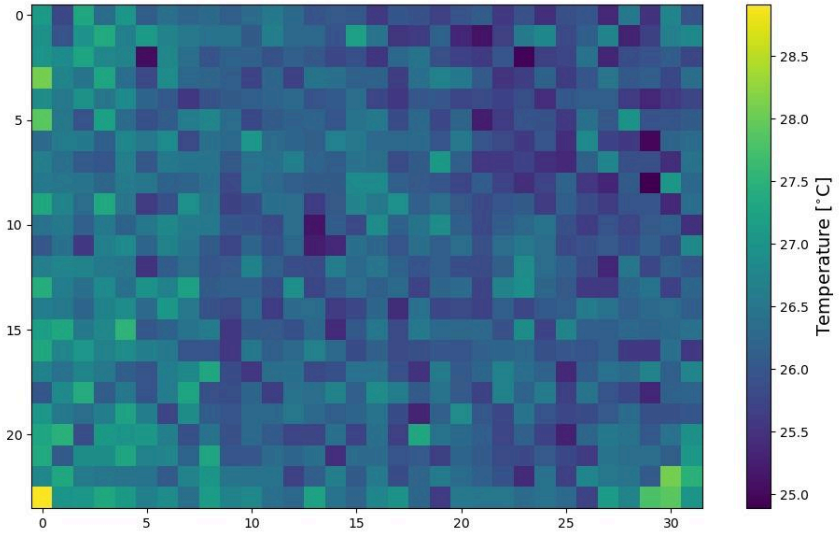

Figure 9: An IR-image of a faulty DUT.

Figure 10 shows the functional DUT photographed 2 minutes after being powered up. Components that do not heat up, or dead space on the board is still roughly the same temperature as the faulty DUT.

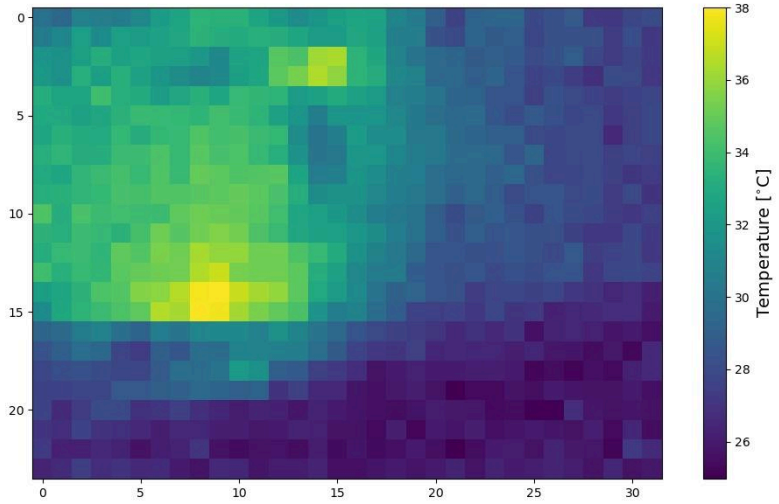

Figure 10: An IR-image of a functional DUT.

The yellow pixels are a clear indication that some components of the DUT are heating up, compared to *figure 9*. Important to notice is that the scale on the right of both pictures has changed. These two pictures show a distinct difference between the two databases that the DNN uses to examine a future DUT.

6.3 DNN for the IR-camera

The 2 databases that are used to train the DNN consist of 80 images of faulty DUTs and 100 images of functional ones. 5 images of both functional and faulty DUTs that are not in the databases are used in order to test the DNN's accuracy. Random images that were not of the DUT were also tested which gave an output that ranged anywhere between 0.2-0.8.

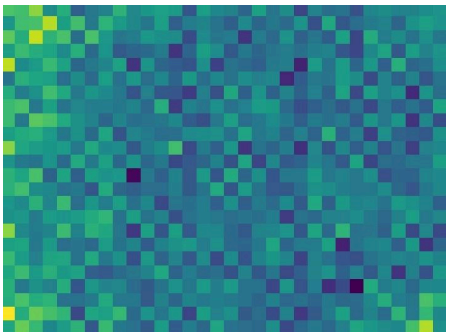

Figure 11 a: faulty image tested

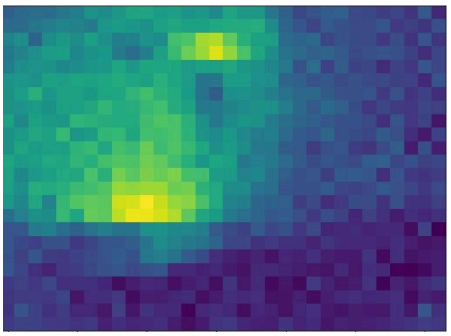

Figure 11 b: functional image tested

The faulty image (*figure 11 a)* resulted in an output of 2.005411e-14 which is very close to 0 that represents the faulty database.

The functional DUT (*figure 11 b)* resulted in 0.9996102, also very close to 1 that represents functional DUTs.

7. Discussion

The original circuit for the magnetic method was designed with instrumental amplifiers, low pass filters and a Teensy 4.1 but was later scrapped in the final design, mainly due to time restrictions. The amplifiers never worked and attempts were made to fix the issue such as matching the input and output impedance as these were highly unbalanced, but due to time restrictions a new design had to be created without them. Wires were soldered directly from the GMRs output to the Teensy, the low pass filters were also skipped due to the difficulty of hand soldering to these small components. During soldering an unexpected problem occurred, a wire accidentally made contact with a coil connecting it directly to the Teensy, making the microprocessor unusable after testing. The problem was quickly fixed by replacing it with an Arduino Uno. The biggest downside to this was the lack of analogue pins that an Arduino Uno had, meaning that only a couple of GMRs could be tested at a time. The integrity of testing quickly dropped after this as changing wires in Arduinos have a high susceptibility to play, greatly disturbing the results and chances of gaining a magnetic signature of some sort. Ontop of that, current carried through a conductor creates a magnetic field which in this circuit causes electromagnetic interference between the wires. Since functional- and faulty device test was done straight after each other, it meant that no wires had to be removed from the Arduino while going from a functional DUT to

a faulty one, the ability to see whether a magnetic signature was obtainable or not was still possible. If the differential voltage between each testing pair was the same at each GMR, a magnetic signature should be possible. *Table 1* shows exactly this and results are promising. Disregarding noise, which again is highly likely given the situation, most GMRs sense a fairly similar output as the DUT goes from turned off to turned on indicating that there is a possibility in creating a magnetic signature.

Test 1 shown in *figure 6* shows a lot of activity when measuring the functional DUT. However, most of this activity is determined to be noise. When a sensor's output signal was not corrupted by noise, such as most GMRs in test 3, seen in *figure 7* and *figure 8*, it shows that the difference between a functional and faulty DUT is minimal, oftentimes only fluctuating by a bit. The minimal difference in output signal was expected, due to the lack of amplification. A lot of information about the change in GMR output is most likely lost due to differences being smaller than what the resolution of the arduino provided.

The neural networks often gave wrong results, most likely due to the similarities in testing pairs. Not having a clear distinction between functioning and faulty magnetic signatures made the neural network confused in what to look for.

The IR–camera that is used has a relatively low resolution compared with what is available today. This means that this thesis is more of a proof of concept, rather than an actual product that can be sold in today's industry. The relatively cheap camera is able to determine if the DUT is functional, but is not capable of showing the heat signature of specific components.

The DNN relies on a large and diverse database. This can be achieved by photographing DUTs with different known faults as well as different functional DUTs. The core function of the DNN is to process a new image and compare it against two databases, one of functional PCBs and one of faulty PCBs, to determine which it more closely resembles. The specific fault in a PCB is not of interest; the important factor is whether the PCB does not match the profile of a functional one. Therefore, it is crucial to develop an extensive database of functional DUTs to ensure accurate results. However, this process can be very time-consuming.

The environment is an important factor when using the thermal imaging method. Ambient temperature, airflow and humidity can play a great part in detecting faults in the DUTs, which is important to know as it can taint the training data and create inconsistencies for future use. This means that using this method in a controlled environment is very important.

The specific DUT tested in this thesis had limitations. The first issue was the limited access to multiple DUTs. Even though they function the same, different DUTs will yield slightly different values. Access to DUTs with different faults instead of using one that is turned off is also a big

benefit since a faulty device may still heat up some components, or yield a magnetic field, and therefore interfere with the results that have not taken this into account.

Another problem is the limited battery time on the DUT. It managed to be powered up for roughly 3 minutes before shutting down and then having to be recharged for almost one hour. To work around this problem, several data samples were collected with minimal time differences, which worsens the variety needed in the databases. These factors are of great importance if these methods are to be used in a commercial aspect where thousands of different PCBs need to be tested.

8. Conclusion

8.1 Can the magnetic signature of a PCB be determined?

Even without amplifiers, the GMR was able to detect activity as the device was turned on but something that resembled a magnetic signature was hard to come by. Results from *Table 1* suggest that there is a possibility in creating a magnetic signature due to the similarity in differential voltage between each test pair for most GMRs, but the components on the sensor card would need to be fixed in order to make this possible.

8.2 Can a thermal signature of a PCB be determined?

Thermal imaging has been a powerful tool for a long time providing an easy way to visualise and interpret data. In determining the status of a PCB, IR-images are also a viable tool. The results showed a clear, recognisable image over several repeated attempts. Although it was not possible to compare this with faulty DUTs where only some components are heated up, the important part is that it can be recognized with the database for functional PCBs.

8.3 Is it possible to classify the status of a DUT using machine learning with the data from magnetic and thermal signatures?

Due to the testing's lack of integrity, it was not possible to classify the status of a DUT using machine learning with data from the GMRs. Either more data was required to perhaps average out a magnetic signature for functioning and faulty devices or create the model that was intended. Perhaps then a neural network would have been a useful tool in classifying the status of a DUT. The IR-images of a functional and faulty PCB are clear enough for the DNN to learn the patterns and determine the functionality of a PCB. For this thesis, it only displays the result as faulty or functional. For future work, creating a more advanced AI will create a considerable difference. If there are a few recurring faults with a PCB, more databases can be created to detect the specific fault. If the fault is a cost-efficient fix, this could save a considerable amount of money.

8.4 Which is the preferred non-contact method?

Both methods have their advantages and disadvantages. The GMR method provides a significantly faster test-system as it does not require the DUT to heat up, potentially saving considerable time depending on the PCB being tested. However, its complex solution introduces

more potential sources for errors. The IR method features a simpler system, and with the use of a high-resolution camera, it can also be enhanced to detect specific faulty components. Its main drawback is building the databases as it requires a broad spectrum of test data to not make errors by misinterpreting a future DUT. Creating these databases involves capturing numerous images and necessitates human supervision, which can substantially increase costs. There is potential in using GMR and this method should definitely be further studied, however, due to the clear results and potential for future improvements, the IR method is currently the preferred method for non-contact PCB fault detection.

9 . References

[1] Electronics Notes. “ICT, in Circuit Test Tutorial”. [Online]. Available: https://www.electronics-notes.com/articles/test-methods/automatic-automated-test-ate/ict-in-circuit-test-what-is-primer.php Accessed: 07-04-2024

[2] JHDPCB. “In-Circuit Testing”. [Online] Available: https://jhdpcb.com/blog/in-circuit-testing/ Accessed: 09-05-2024

[3] Daniel Bengtsson, Wiktor Löw (2020). Non-Contact PCB Fault Detection Using Near Field Measurements and Thermal Signatures.” https://www.diva-portal.org/smash/get/diva2:1446564/FULLTEXT01.pdf

[4] Nabil El Belghiti Alaoui, Alexandre Boyer, Patrick Tounsi, Arnaud Viard. New defect detection approach using near electromagnetic field probing of high density PCBAs, Microelectronics Reliability, 2018, https://www.sciencedirect.com/science/article/pii/S0026271418306498

[5] Z. Wang, H. Yuan, J. Lv, C. Liu, H. Xu and J. Li, "Anomaly Detection and Fault Classification of Printed Circuit Boards Based on Multimodal Features of the Infrared Thermal Imaging," in *IEEE Transactions on Instrumentation and Measurement, 2024, https://ieeexplore.ieee.org/abstract/document/10494238*

[6] Britannica. "Magnetic field physics" [Online]. Available: https://www.britannica.com/science/magnetic-field Accessed: 17-04-2024

[7] Chang, L., Wang, M., Liu, L., Luo, S., & Xiao, P. (2014). “A brief introduction to giant magnetoresistance” https://arxiv.org/abs/1412.7691 pp.2

[8] Ouyang, Yong & Jinliang, He & Hu, Jun & Wang, Shan. (2012). A Current Sensor Based on the Giant Magnetoresistance Effect: Design and Potential Smart Grid Applications. Sensors (Basel, Switzerland), pp.15523

https://www.researchgate.net/publication/233828535_A_Current_Sensor_Based_on_the_Giant_Magnetoresistance_Effect_Design_and_Potential_Smart_Grid_Applications

[9] Nasa. “Infrared Waves”. [Online]. Available: https://science.nasa.gov/ems/07_infraredwaves/

Accessed: 17-04-2024

[10] Robocraze. “IR Sensor Working” [Online]. Available: https://robocraze.com/blogs/post/ir-sensor-working Accessed: 15-04-2024

[11] Infratec. “What is a Thermal Camera”. [Online]. Available: https://www.infratec-infrared.com/thermography/service-support/glossary/infrared-camera/#:~:text=A%20thermal%20camera%20%E2%80%93%20also%20called,the%20surface%20temperature%20of%20objects Accessed: 15-04-2024

[12] Fluke Co.. “What is Thermal Imaging? How a Thermal Image is Captured”. [Online]. Available: https://www.fluke.com/en/learn/blog/thermal-imaging/how-infrared-cameras-work Accessed: 15-04-2024

[13]IBM. “What is a Neural Network?”. [Online]. Available: https://www.ibm.com/topics/neural-networks Accessed: 11-04-2024

[14] Cristian Musuroi, Mihai Oproui, Marius Volmer, Jenica Neamtu, Marioara Avram, Elena Helerea. (2021). “Low Field Optimization of a Non-Contacting High-Sensitivity GMR-Based DC/AC Current Sensor”. https://www.mdpi.com/1424-8220/21/7/2564 pp. 3-10.

[15] NVE Corporation. “GMR Analog Sensor Datasheet”. [Online]. Available: https://www.nve.com/Downloads/analog_catalog.pdf Accessed: 07-04-2024